A Critical Analysis of Linear Inverse Solutions to the Neuroelectromagnetic Inverse Problem

Rolando Grave de Peralta-Menendez* and Sara L. Gonzalez-Andino

***Abstract*—This paper explores the possibilities of using linear inverse solutions to reconstruct arbitrary current distributions within the human brain. We formally prove that due to the underdetermined character of the problem, the only class of measurable current distributions that can be totally retrieved are those of minimal norm. The reconstruction of smooth or averaged versions of the currents is also explored. A solution that explicitly attempts to reconstruct averages of the current is proposed and compared with the minimum norm and the minimum Laplacian solution. In contrast to the majority of previous analysis carried out in the field, in the comparisons, we avoid the use of measures designed for the case of dipolar sources. To allow for the evaluation of distributed solutions in the case of arbitrary current distributions we use the concept of resolution kernels. Two summarizing measures, source identifiability and source visibility, are proposed and applied to the comparison. From this study can be concluded: 1) linear inverse solutions are unable to produce adequate estimates of arbitrary current distributions at many brain sites and 2) averages or smooth solutions are better than the minimum norm solution estimating the position of single point sources. However, they systematically underestimate their amplitude or strength especially for the deeper brain areas. Based on these result, it appears unlikely that a three-dimensional (3-D) tomography of the brain electromagnetic activity can be based on linear reconstruction methods without the use of a significant amount of *a priori* information.**

***Index Terms*—Electromagnetic tomography, linear inverse solutions, neuroelectromagnetic inverse problem, source localization.**

I. Introduction

THE core of the neuroelectromagnetic inverse problem (NIP) is the determination of the neuronal current distribution within the brain, on the basis of the electroencephalogram (EEG) and/or the magnetoencephalogram (MEG). The existence of silent sources, i.e., sources that produce nonmeasurable fields on the scalp surface [1] determines its severely ill-posed character. Additionally, the number and the quality of the measurements are insufficient to provide a precise reconstruction of arbitrary current distributions. This demands the incorporation of strong assumptions about the character of the currents, e.g., few dipolar sources [2], in the reconstruction procedure. When more complex distributed currents are likely to occur, e.g., in higher brain functions, a sensible approach is the use of linear reconstruction methods [3]–[6], in an attempt to construct a three-dimensional (3-D) tomography of the neural sources. The main purpose of this work is to investigate the feasibility of obtaining this tomography with linear reconstruction methods under ideal conditions (exact data).

The NIP differs from other modalities of medical imaging [e.g., positron emission tomography (PET) and single photon emission computed tomography (SPECT)], in that the spatial resolution of EEG (MEG) data is very low. The number of independent measurements that can be obtained is limited and, thus, this inverse problem is intrinsically underdetermined. In the case of underdetermined linear inverse problems only a finite amount of information about the unknown parameters can be derived, even in the ideal case of infinitely precise measurements [7]. This limitation implies that there are classes of sources that cannot be retrieved by a given linear reconstruction method, restricting the applicability of these algorithms. In spite of these limitations, useful solutions could be obtained if the physical properties of the problem permit the estimation of averaged or blurred versions of the actual neural sources. In this paper, a solution based on the estimation of averages is proposed and the possibility of obtaining a blurred tomography of the sources using either this solution or a linear solution that attempts the smoothest reconstruction of the currents is investigated.

In Section II, following a brief statement of the NIP, the concept of model resolution matrix [8] is introduced as the basis to evaluate linear inverse solutions. Two measures, the source visibility and the source identifiability, are then defined to evaluate the expectable and the achievable quality of the reconstructions that can be provided by linear inverse solutions. After that, an exposition of some theoretical limitations of linear methods follows and finally some elements of Backus–Gilbert formalism [7] are introduced to justify the proposal of a solution based on averages. Section III deals with computer simulations carried out to evaluate the possibility of achieving a 3-D tomography based on linear reconstruction methods. The mathematical details considering the general theoretical framework for deriving linear inverse solutions and the lemma that proves their basic theoretical limitations are left to the Appendixes. Throughout this paper, uppercase and lowercase bold letters represent matrices and vectors, respectively, and $\mathbf{X}^t$, $\mathbf{X}^{-1}$, $\mathbf{X}^+$, and $\|\mathbf{X}\|$ denote the

Manuscript received September 19, 1996; revised November 7, 1997. This work was supported in part by a grant from the Deutsche Forschungsgemeinschaft (Klinische Forschergruppe "Biomagnetismus and Biosignalanalyze") and by the Swiss National Foundation under Grant 4038-044081/1. *Asterisk indicates corresponding author.*

*R. Grave de Peralta-Menendez is with the Functional Brain Mapping Laboratory, University Hospital Geneva, 24 rue Michel-du-Crest, 1211 Geneva 14, Switzerland (e-mail: grave@diogenes.hcuge.ch).

S. L. Gonzalez-Andino is with the Functional Brain Mapping Laboratory, University Hospital Geneva, 1211 Geneva 14, Switzerland.

Publisher Item Identifier S 0018-9294(98)01795-9.

transpose, the inverse, the Moore–Penrose pseudo inverse, and the norm of $\mathbf{X}$, respectively.

II. Methods

A. Basic Theory

The relationship between fields measured on the scalp surface $\mathbf{m}$ and their sources, the primary current density $\mathbf{j}$, can be expressed for the discrete problem through the lead field concept $\mathbf{L}$ [9]

$$\mathbf{m} = \mathbf{L}\mathbf{j} \tag{1}$$

where vector $\mathbf{j}$ $(3N_p \times 1)$ is composed of the x, y, and z components of the primary current in the N_p grid points, and vector $\mathbf{m}$ contains the N_m measured data. The lead field matrix $\mathbf{L}(N_m \times 3N_p)$ reflects the sensitivity of the sensors to the sources and depends on the geometry and conductivities of the volume conductor model used to describe the head. Its elements $\mathbf{L}_{i,3(p-1)+1}$, $\mathbf{L}_{i,3(p-1)+2}$, and $\mathbf{L}_{i,3(p-1)+3}$ represent the sensitivity of the ith sensor to the x, y, and z components of $\mathbf{j}$ at the pth grid point.

In practice, $N_m \ll N_p$ and the problem is highly underdetermined. Thus infinitely many solutions exist to (1) and several approaches can be used to yield a unique solution. Many of the approaches which lead to linear inverses can be analyzed using an identical variational formalism described in Appendix I. Examples of some of the linear solutions which have been applied to the NIP are also given. What is common to all of them is that the estimated current density is obtained as the product of a matrix $\mathbf{G}$ times the data vector $\mathbf{m}$, i.e.

$$\hat{\mathbf{j}} = \mathbf{G}\mathbf{m} = \mathbf{G}\mathbf{L}\mathbf{j}. \tag{2}$$

B. The Resolution Matrix as a Measure of the Effectiveness of the Different Source Reconstruction

The product $\mathbf{R} = \mathbf{GL}$ that appears in (2) is known as the model resolution matrix [8], [10] and provides a powerful tool to analyze the performance of the inversion procedure $\mathbf{G}$ in the reconstruction of $\mathbf{j}$, in the absence of noise. The interpretation of its rows (the resolution kernels) and its columns (impulse responses) is briefly presented here. For more details about this interpretation or applications of $\mathbf{R}$ to the analysis and/or comparison of linear inverse solutions, see [10] and [11].

1) Resolution Kernels: Each component k of the estimated vector $\hat{\mathbf{j}}$ is associated with a resolution kernel that describes the form in which other components of $\mathbf{j}$ affect its reconstruction. Since the estimated solution $\hat{\mathbf{j}}^k(r_p)$ is a linear combination of the true distribution with coefficients given by the ith row of $\mathbf{R}$ $(i = 3(p-1)+k,\ k = 1, 2, 3)$, this row describes how the different components of the true current distribution are averaged by the solution $\mathbf{G}$ to provide the estimated solution. Note that it follows from this definition that the resolution kernels are independent from any particular source model assumed for $\mathbf{j}$. Specifically, if for some point r_p the resolution kernel is centered at r_p, strongly peaked near r_p and small elsewhere, then a source at that point can be independently predicted or resolved from the available data and the resolution kernel is considered to be a localized average [8]. In practice, resolution kernels may exhibit large sidelobes, wildly oscillating behaviors, or may be incorrectly centered which confuse the interpretation of the resolution concept [11].

2) Impulse Responses: The columns of $\mathbf{R}$ are useful to evaluate the ability of a given solution $\mathbf{G}$ to retrieve single point sources. If the actual source distribution coincides with a single point source of unitary strength at grid point r_p, then the solution provided by the algorithm $\mathbf{G}$ in the absence of noise is identical with the ith column of $\mathbf{R}$ $(i = 3(p-1)+k,\ k = 1 \cdots 3)$. The amplitude of the main peak of a column could be interpreted as the amplification or reduction produced by the inverse $\mathbf{G}$ when a single point source actually exists at that point whereas the width of the main peak as the smearing. All the nondiagonal values are ghost or spurious sources produced by the inversion procedure $\mathbf{G}$.

In the analysis of the realistic situation, where the current distribution may be arbitrary, the resolution kernels are crucial. The information contained on the impulse responses concerns exclusively single point sources, a situation which does not correspond to the aims of linear distributed inverse solutions. Thus, the performance of linear distributed solutions in the presence of arbitrary current distributions cannot be adequately evaluated on the basis of impulse responses or measures derived from them.

C. Source Identifiability and Source Visibility

Linear reconstruction techniques as the ones discussed here promise to characterize, in principle, sources of arbitrary extent or shape. However, the performance of these methods is usually evaluated using a finite number of dipoles as the source model and then applying measures such as the dipole localization error (DLE). Using dipoles to evaluate the performance of these methods is understandable, since dipoles are the easiest implementable source model. However, the evaluation of these methods exclusively in terms of DLE is questionable. This analysis takes into account, neither the estimated value for the source amplitude (strength) nor the possible existence of simultaneously active sources. In addition, note that the superposition principle does not apply to nonlinear magnitudes such as the DLE.

As discussed above, the analysis of linear methods in terms of its resolution kernels takes all these aspects into account. Nevertheless, for fine source space discretizations the whole analysis of the resolution kernels might be infeasible and it is easier to summarize this information using some figures of merit [10]. Here, we propose one figure which partially evaluates the quality of a resolution kernel at every solution point. This measure, termed source identifiability, takes into account that a "good" resolution kernel has to be correctly centered and has to have an amplitude of one at the main peak. If the value of the resolution kernel at a grid point is nearly zero, a source at that point will be hardly retrieved. This measure is defined for each component k of the estimated $\hat{\mathbf{j}}$, as

$$I_k = \frac{(D - d_{ki})\mathbf{R}_{kk}}{D}$$

where D represents the maximum distance between grid points, $\mathbf{R}_{kk}$ denotes the absolute value of the kth element of the kth row of $\mathbf{R}$ (the diagonal element), and d_{ki} is the Euclidean distance between the grid point associated with this row and the point (r_i) where the maximum value of the kth row was found. According to this definition, a high value of I indicates that the activity at this point can be correctly retrieved by the algorimthm $\mathbf{G}$, independently of the spatial blurring. A value near zero expresses either that the main peak is far away from the target point or that the amplitude of the resolution kernel at the point is small. Both undesirable features result in poor identifiability of the current distribution.

To further illustrate the practical consequences of the underdetermined character of the NIP, we introduce here a second figure of merit, termed source visibility. The visibility of a source (V_i) evaluates as to what extent an arbitrary current distribution can be detected by the sensor configuration. It is defined as the ratio between the size of the visible part and the size of the source. For single point sources, it is given by $V_i = \|\mathbf{L}^+\mathbf{L}_i\|^2$ where $\mathbf{L}_i$ is the ith column of the lead field matrix. Note that the identifiability depends on the inverse $\mathbf{G}$, i.e., on the *a priori* information added to the problem whereas the visibility is defined only in terms of the lead field matrix. This measure might be used to evaluate a given sensor configuration or to compare measurement techniques (e.g., EEG and MEG).

D. Some Fundamental Limits in Underdetermined Inverse Problems

The underdetermined character of the discrete NIP set limits not only in the spatial resolution of the reconstruction of the currents [8], [11], [12], but also in the class of nonsilent current distributions that can be retrieved by an arbitrary linear reconstruction algorithm $\mathbf{G}$. In practical terms, it is impossible to reconstruct the detailed shape of arbitrary primary current distributions from finite data, i.e., it is impossible to give accurate values for the primary currents at arbitrarily selected grid points. Since any underdetermined inverse problem is characterized by a resolution matrix $\mathbf{R}$ different from the identity matrix, the estimates provided by any linear solution are, in the best case, localized averages of the actual current distribution [8]. Accordingly, attempts to estimate the exact value of the unknown $\mathbf{j}$ at every grid point using linear inverse solutions are sterile.

Still, one can hope that by using some reasonable *a priori* information about the sources (e.g., maximum smoothness [5]) to construct the linear inverse, we can adequately retrieve all the sources that agree with the *a priori* information. The lemma given in Appendix II proves that this is not possible. For any linear inverse solution different from the minimum norm and which explains the data, this lemma identifies the class of sources that cannot be retrieved. In simple words, it expresses that with the exception of the minimum norm, all linear inverse solutions will fail retrieving some of the measurable source configurations that fulfill a certain property. This occurs even if the inverse solution is conceived to deal with this type of sources. For instance, although the ML solution [5] is intended to deal with smooth source distributions, it is unable to retrieve constant or smooth current distributions that reach the maximum at the borders of the solution grid, e.g., $J(x,y,z) = (x^2,y^2,z^2)$. Thus, current distributions with maxima at the borders of the cortical mantle will be inadequately retrieved.

E. A Solution Based on Averages

In the cases where no additional *a priori* information about the sources is available, a natural constraint posed by the underdetermined character of the NIP is the estimation of averages of the current density at each solution point. The problem of estimating averages or mollifiers of the unknown parameters has been considered in other fields of application of inverse problem (see [13], [14], and references therein). However, in these cases, there was no attempt to restore the original parameters and, thus, these solutions were not consistent with the data. In contrast, in the approach presented here, the goal is to obtain a data consistent solution using as *a priori* information the fact that nothing but averages of the true sources can be reconstructed, i.e., we look for

$$\mathbf{j}_{\text{ave}} = \mathbf{A}\mathbf{j} \tag{3}$$

where the rows of $\mathbf{A}$ represent the averages (linear combinations) of the true sources. In this way the metric matrix $\mathbf{W}_m$ is defined in an intuitive form ($\mathbf{W}_m = \mathbf{A}^t\mathbf{A}$) which is consistent with the *a priori* information available. If $\mathbf{A}$ is invertible an estimate $\hat{\mathbf{j}}$ of the original parameters, consistent with the data, can be obtained

$$\hat{\mathbf{j}} = (\mathbf{A}^t\mathbf{A})^{-1}\mathbf{L}^t\left[\mathbf{L}(\mathbf{A}^t\mathbf{A})^{-1}\mathbf{L}^t\right]^{-1}\mathbf{M}. \tag{4}$$

Many different averages can be constructed, and the inverse solution will depend on the specific form of $\mathbf{A}$. Nevertheless, the only averages that can be correctly identified are those that can be represented as a linear combination of the rows of $\mathbf{L}$. Physically, an average makes more sense if it contains only positive weighting factors that decay with the distance to the target element [8]. One alternative is to consider averages that can be tuned to produce more or less smoothed versions of the delta function (a single point source). In the definition of the elements of the averaging matrix that follows, the subscript p,q is used to indicate grid points and the subscript k,m is used to represent the Cartesian coordinates x, y, and z (i.e., $k,m = 1$, 2, and 3). An element of matrix $\mathbf{A}$ is given by

$$\begin{aligned} A_{ij} &= A_{3(p-1)+k,3(q-1)+m} \\ &= w_j e^{-\left(\frac{d_{pq}^2}{\sigma_i^2}\right)} \quad \text{for } k = m \text{ and zero otherwise.} \end{aligned} \tag{5}$$

where d_{pq} represents the Euclidean distances between the pth and qth grid points. The coefficients w_j can be used to describe a column scaling by a diagonal matrix. Note that, by changing the values of σ_i and w_j, it is possible to obtain the minimum norm solution (MN) ($\sigma_i \to 0$, $w_j = 1$) or any particular case of weighted MN ($\mathbf{W}_m$ diagonal). In the limit case, $\sigma_i \to \infty$, all the rows of $\mathbf{A}$ are identical, thus only one average of the true sources is reconstructed. In this case, $\mathbf{A}$ is not invertible and (4) cannot be used (see [15] for the general solution). The

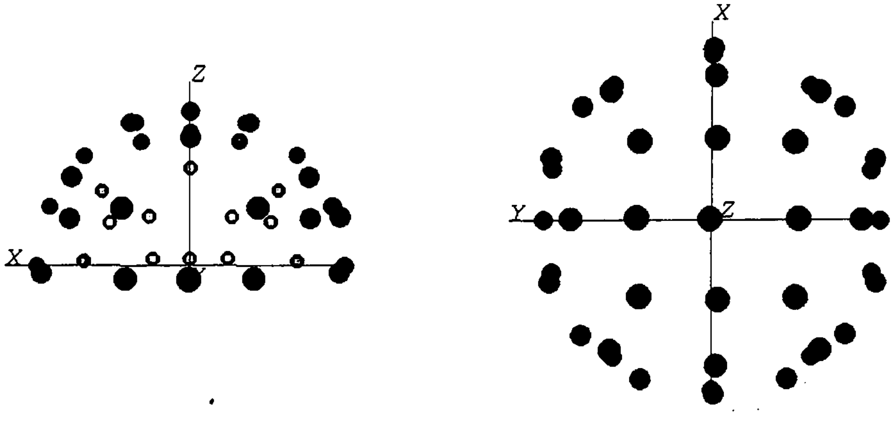

Fig. 1. Sensor configuration from two different viewpoints. (a) View from the right; (b) view from the top. The dots represent the 41 electrodes distributed on the upper half of the most external unitary radius sphere. Coordinate system used in the following plots is indicated in this figure.

spatial resolution, i.e., the size of the neighborhood considered in the average, depends upon the σ_i values which can be either adjusted globally or for each point individually. An increase in the values of σ_i is equivalent to consider a locally coarser grid and, accordingly, this solution permits variable spatial resolution. With a suitable selection of the averaging neighborhood, the method can be applied to arbitrary source spaces (e.g., the cortical surface). Considerable computational effort can be saved if the matrix **A** can be expressed in terms of a Kronecker product, e.g., assigning the same value of σ for all the averages associated to one point.

III. Computer Simulations

A. General

The limits to the reconstruction, described in Section II-D, are inherent to any underdetermined linear reconstruction method, independently of the physical character of the particular inverse problem. In spite of these limitations, averaged [14] or smooth reconstructions [16] of the original parameters have proved to be useful in other fields of applications. In this section, we analyze by means of computer simulations, how the described theoretical limitations will affect the reconstruction of arbitrary current distributions in the case of electrical measurements. For that purpose, the MN is compared here with the averaged solution (AS) and the minimum Laplacian solution (ML). The basis for the comparison and analysis are the figures of merit described in Section II-C and their resolution kernels. Note that, the following comparisons are data independent since they are based on the concept of the model resolution matrix.

The matrix **A** of the AS was constructed using a constant value of $\sigma = 0.02$ and the coefficients w_j were selected using a radial weighting strategy described in Appendix III.

The model resolution matrix associated with each solution was constructed considering the case of electric measurements. To simplify the calculations, a three layer spherical model with radius and conductivities as described in [17] was used. A set of 41 electrodes was distributed on the surface of the upper half sphere as represented in Fig. 1. A regular cubic grid of 1152 solution points with minimum intergrid distance $d = 0.133$ was confined to the upper half inner sphere volume.

B. Simulation Results

The number of solution points considered in this study, impede a detailed exposition of all the resolution kernels and the impulse responses associated with each solution. Roughly, the observed behavior of the resolution kernels and the impulse responses can be classified according to one of the categories illustrated in Fig. 2: 1) Well-resolved resolution kernels (impulse responses) with narrow high peaks correctly centered at the target point and almost missing sidelobes. 2) Resolution kernels (impulse responses) strongly peaked at points far from the target point and with very low amplitude at the target point. 3) Resolution kernels (impulse responses) with very small amplitudes everywhere, wildly oscillating around the zero level. The main difference observed was that the number of adequately centered impulse responses (although with very low amplitude) was higher for the ML and the AS than for the MN This suggests that a better estimation of the position of single point sources can be obtained but underestimating the source strength due to the low amplitude of the impulse responses at the target point. Single point sources at such points could be "detected" only when their strength is remarkably higher than that of other simultaneously active sources. In this case, a better performance of ML and AS should be expected. The presence of noise in the data or the existence of simultaneously active sources with similar amplitude but with better impulse responses (first category) will make impossible to discriminate such sources in the reconstructed maps.

In terms of the resolution kernels, no significant difference was observed among the solutions. For the majority of the points of the solution grid the resolution kernels belong to the third of the categories described before. This can be noted in the plots of the source identifiability presented in Fig. 3. Since no significant difference was found among the x, y and z components of the sources we present only the source identifiability for z. It is evident that the three plots are remarkably similar and that the identifiability of the sources

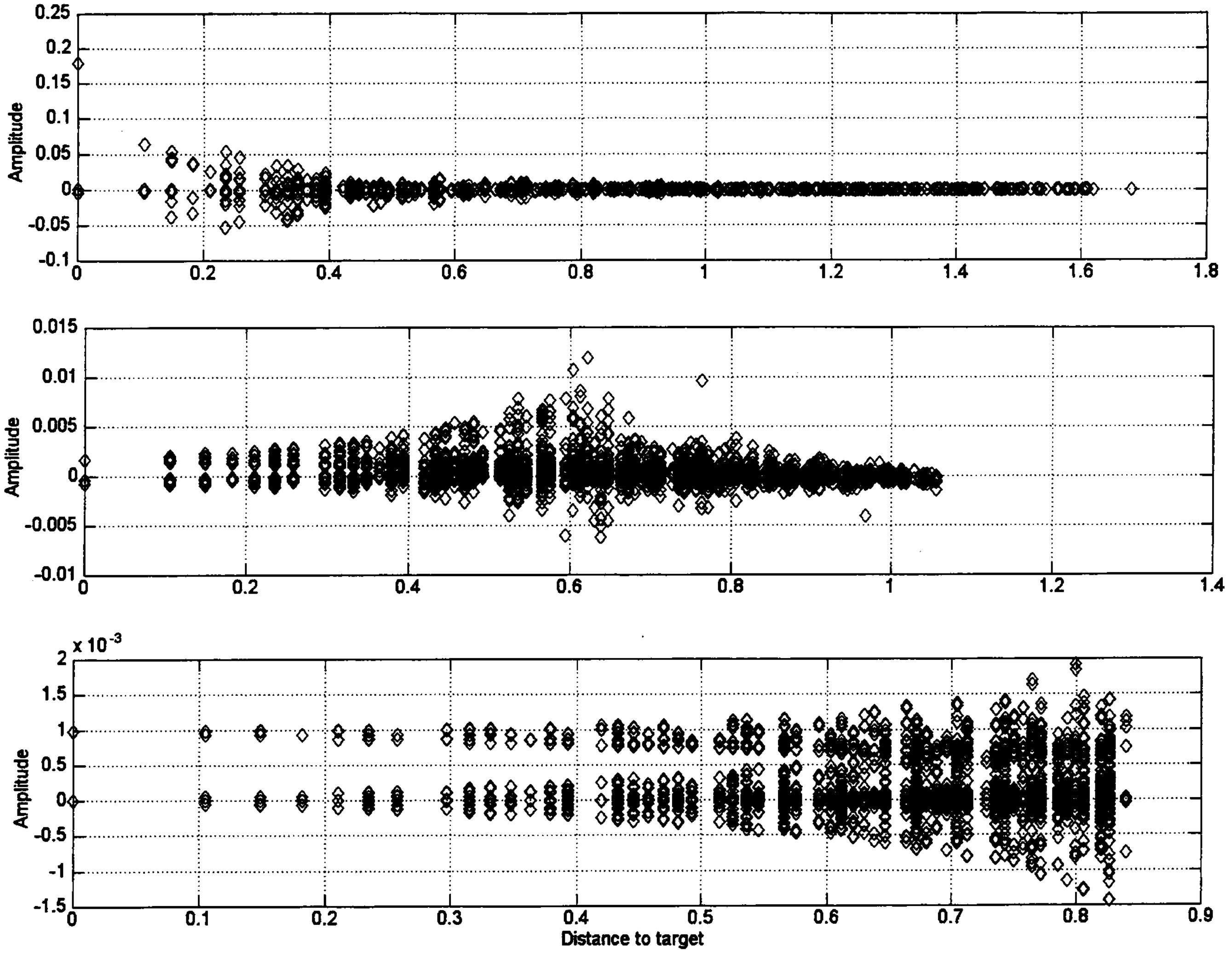

Fig. 2. Different categories of resolution kernels as described in the text. In the horizontal axis the points are organized according to their Euclidean distance to the target point.

decreases with the depth of the points. The fact that this reduction approximately occurs at the same depth for all three solutions confirms once more that mainly eccentric sources, i.e., cortical sources, can be identified. From the definition of identifiability, the resolution kernels associated with sources having a low identifiability are either incorrectly centered (maximum far from the target point) or/and with very low amplitude at the target point. In such cases, the estimates yield insufficient information about the activity at the point or its vicinity. Thus, not even a blurred reconstruction seems to be possible for such locations, especially if other regions are simultaneously active.

The *a priori* information used in AS or ML can slightly improve the quality of the impulse responses, but not that of the resolution kernels. This is due to the fact that the columns of $\mathbf{R}$ (impulse responses) are linear combinations of the columns of the inverse $\mathbf{G}$. In contrast, the rows of $\mathbf{R}$ (resolution kernels) are linear combinations of the rows of the lead field matrix $\mathbf{L}$. While the inverse can be conveniently selected to determine the space to which the impulse responses belong, the same is not true for the resolution kernels. Since the resolution kernels are constrained to the space spanned by the rows of $\mathbf{L}$, they are (although dependent on the *a priori* information) intrinsically determined by the physical laws relating sources to measurements and the experimental design (sensor and grid point locations). In contrast, the impulse responses are determined by the *a priori* information added. Hence, the quality of the impulse responses (or measures derived from it, e.g., the dipole localization error) does not depend on the source·location but on the *a priori* information used to construct the inverse $\mathbf{G}$. By means of constrained inverses [15], it is always possible to obtain N_m ideal impulse responses (assuming that the reference for the potential is known), i.e., to force the dipole localization error to be zero for these N_m arbitrary sources independently of their location. However, resolution kernels cannot be "manipulated" at will. This suggests that while it is possible to improve the capabilities of linear inverse solutions for the estimation of the position of single point sources the same does not hold for arbitrary current distributions.

The extent of the underdetermined character of the problem for a given finite set of measurements can be evaluated using the plots of the source visibility as in Fig. 4. It is evident that the dependence of the visibility with source depth is similar

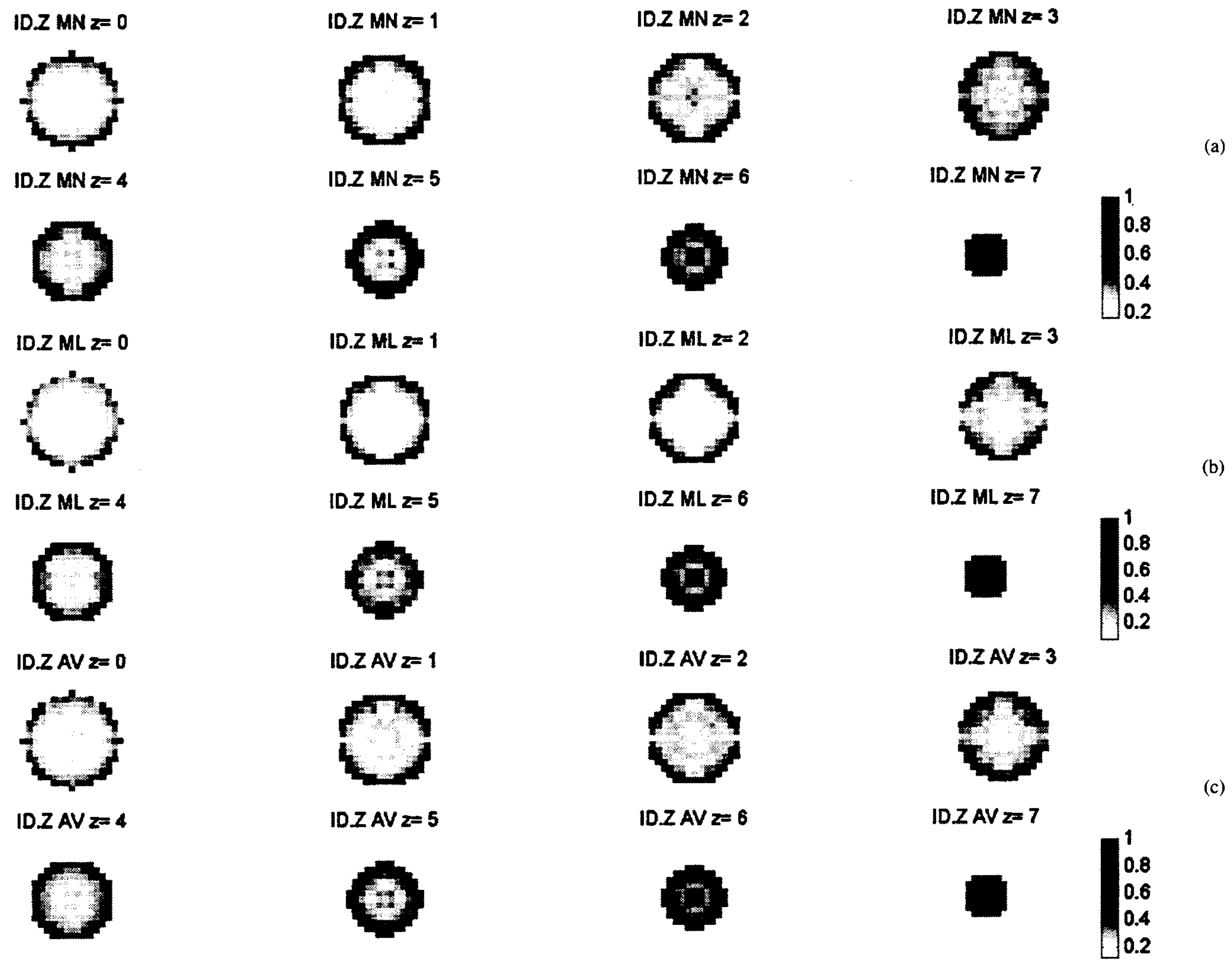

Fig. 3. Plots of source identifiability for the z-component of a source at every solution point. The lower slice ($z = 0$) corresponds to the horizontal plane at the middle of the unitary sphere and the values of z are indicated at the top of each slice. (a) MN, (b) ML, and (c) AS.

to that observed in Fig. 3, suggesting that identifiability and visibility are closely related concepts. In absence of *a priori* information, the visibility and the identifiability are almost identical. It is clear that the global *a priori* information used by the linear solutions analyzed here is not sufficient to overcome the lack of visibility of the deeper sources. As stated by Lanczos: "A lack of information cannot be remedied by any mathematical trickery." The lack of visibility of the deepest sources can be only compensated by including additional information about them. Note also the existence of points with low visibility near the cortical mantle.

IV. Conclusion

This paper exposed some of the basic limitations of linear solutions in the reconstruction of arbitrary current distributions inside the brain. The theoretical results discussed in Section II prove that a limited number of data is insufficient to determine exactly even those current distributions that fulfill a certain main property that the specific linear solution is intended to cope with. The cornerstone to analyze the influence of these limitations in the estimated solutions is the model resolution matrix. The results of this study clearly show that the estimation of the positions of single point sources can be improved. However, the same cannot be said about the performance of these solutions in the presence of arbitrary current distributions as evident from the analysis of the resolution kernels. The behavior of the solutions presented here seems to be similar for arbitrary source distributions. The identifiability of deep sources remains a challenge for any linear solution. In the more realistic case of noise contaminated data, the problem will be even worse. Still, these solutions could provide practically useful results if poorly identifiable points can be excluded from the grid on the basis of some *a priori* information, e.g., that the generators are restricted to the cortical mantle or if only a few dipolar generators are known to be present. A combination of the resolution matrix with neuroanatomical images could lead to maps that evaluate *a priori*, i.e., without the necessity of performing experiments, the "reliability" of the current reconstruction that will be provided by a particular linear method. Further work in this direction is needed.

On the other hand, the current distributions that can be reconstructed in the NIP are not only limited by the quantity and quality of the data, but also by the physical properties

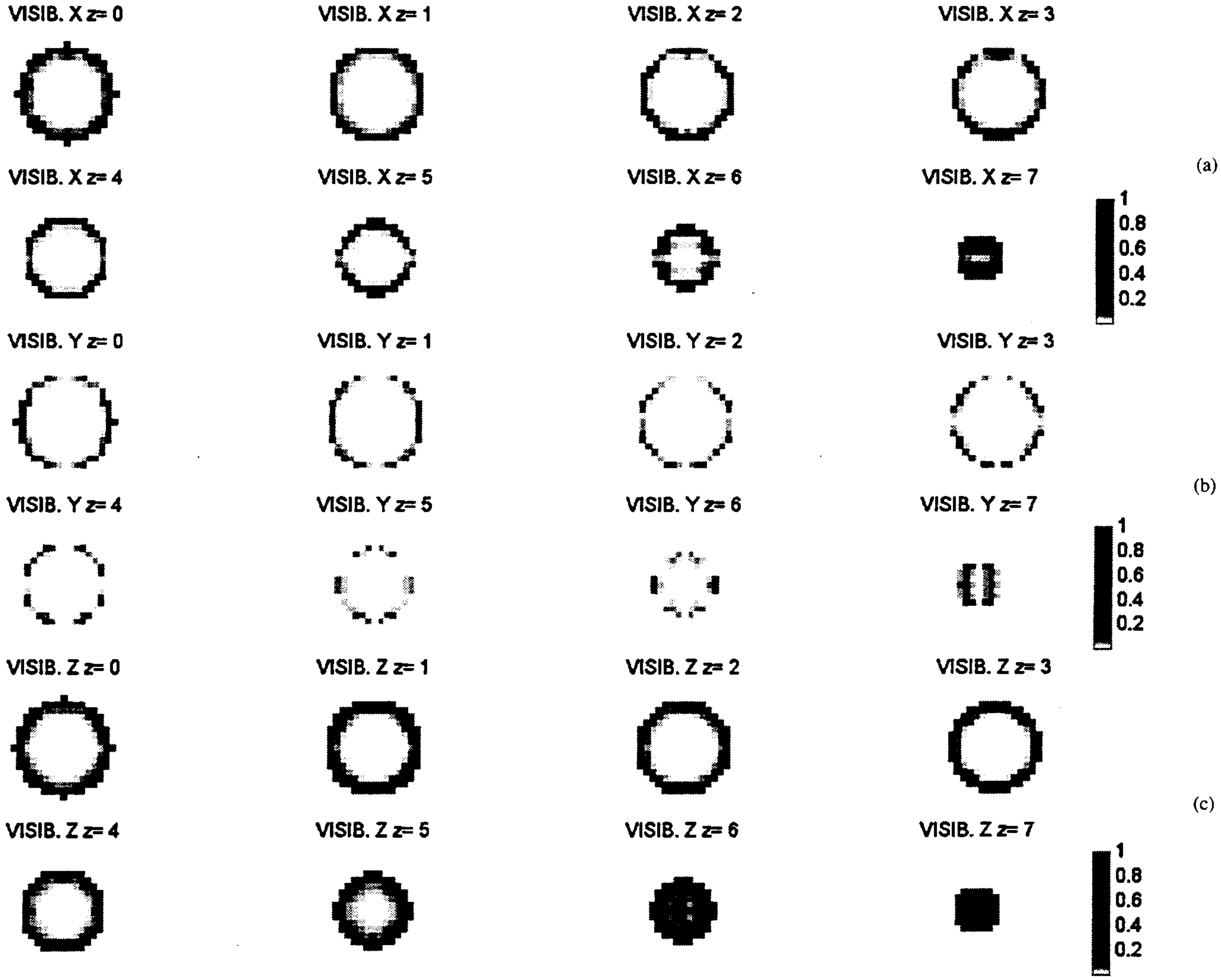

Fig. 4. Plots of source visibility for the (a) x-component, (b) y-component, and (c) z-component of a source at every point of the solution space.

of the measurements. Maxwell equations state that electric measurements contain no information about the solenoidal part of the current densities [18]. Consequently, attempts to estimate the whole vector from EEG data are in vain. Approaches that considerably reduce the dimension of the problem are either to estimate the scalar field $\mathbf{I} = \text{div}\mathbf{J}$, or the potential distribution in depth which are responsible for the generation of the electric potentials measured on the scalp surface.

Appendix I

Several of the approaches that can be used to yield a unique solution to the problem stated in (1) converge to the following variational problem for $\mathbf{j}$ [8]:

$$\min(\mathbf{Lj}-\mathbf{m})^t\mathbf{W}_e(\mathbf{Lj}-\mathbf{m})+\lambda^2(\mathbf{j}-\mathbf{j}_p)^t\mathbf{W}_m(\mathbf{j}-\mathbf{j}_p). \quad \text{(AI-1)}$$

In (AI-1) $\mathbf{W}_e$ and $\mathbf{W}_m$ are symmetric positive (semi) definite matrices representing the (pseudo) metrics associated with the measurement space and the source space respectively. Vector $\mathbf{j}_p$ denotes any *a priori* value of the unknown current density available, e.g., from other modalities of neurofunctional images. The regularization parameter is denoted by λ. Assuming linear independence of the rows of $\mathbf{L}$, the solution to (AI-1) is unique if the null spaces of $\mathbf{W}_m$ and $\mathbf{W}_e\mathbf{L}$ intersect trivially, i.e., $\text{Ker}(\mathbf{W}_m)\cap\text{Ker}(\mathbf{W}_e\mathbf{L}) = \{0\}$. In this case, the estimated solution vector $\hat{\mathbf{j}}$ is given by

$$\hat{\mathbf{j}} = \mathbf{j}_p + \left[\mathbf{L}^t\mathbf{W}_e\mathbf{L} + \lambda^2\mathbf{W}_m\right]^{-1}\mathbf{L}^t\mathbf{W}_e\left[\mathbf{m} - \mathbf{Lj}_p\right]. \quad \text{(AI-2)}$$

When the metric matrices $\mathbf{W}_m$ and $\mathbf{W}_e$ are positive definite (AI-2) is equivalent to

$$\hat{\mathbf{j}} = \mathbf{j}_p+\mathbf{W}_m^{-1}\mathbf{L}^t\left[\mathbf{LW}_m^{-1}\mathbf{L}^t + \lambda^2\mathbf{W}_e^{-1}\right]^{-1}\left[\mathbf{m} - \mathbf{Lj}_p\right]. \quad \text{(AI-3)}$$

In the case of null *a priori* estimates of the current distribution ($\mathbf{j}_p = 0$) and perfectly accurate data ($\lambda = 0$), (AI-3) reduces to

$$\hat{\mathbf{j}} = \mathbf{W}_m^{-1}\mathbf{L}^t\left[\mathbf{LW}_m^{-1}\mathbf{L}^t\right]^{-1}\mathbf{m}. \quad \text{(AI-4)}$$

Equation (AI-4) is a particular case of the class of solutions of (1) that can be expressed by $\hat{\mathbf{j}} = \mathbf{CL}^t[\mathbf{LCL}^t]^{-1}\mathbf{m}$ with $\mathbf{C}$ not necessarily being invertible. Matrix $\mathbf{C}$ can be interpreted in terms of a metric as in (AI-4) or alternatively as a change of variables [19] or as an expansion in basis functions [20].

When $\mathbf{C}$ is invertible the solutions are optimal in the sense that they are the solutions of (1) with minimum $\mathbf{J}^t\mathbf{C}^{-1}\mathbf{J}$. In this class of C-generalized MN's it is assumed that there exist a bound ε for a certain property of the solution that can be expressed by means of matrix $\mathbf{C}$, i.e., $\mathbf{J}^t\mathbf{C}^{-1}\mathbf{J} \leq \varepsilon$. Note that the solution obtained for a given $\mathbf{C}$ does not necessarily belong to the space spanned by the rows of $\mathbf{L}$. Therefore, it can contain silent or invisible sources. This remark makes clear that the selection of the matrix $\mathbf{C}$ must be suggested by sound *a priori* physical considerations [12].

Defining $\mathbf{G} = \mathbf{W}_m^{-1}\mathbf{L}^t[\mathbf{L}\mathbf{W}_m^{-1}\mathbf{L}^t]^{-1}$ as the generalized inverse that in some sense solves the inverse problem and using (1), (AI-4) can be rewritten as

$$\hat{\mathbf{j}} = \mathbf{G}\mathbf{m} \qquad \text{(AI-5)}.$$

A wide class of linear solutions can be constructed following this methodology. In general, different selections of $\mathbf{W}_e$ and $\mathbf{W}_m$ will produce different solutions (See [15] about pairs of norms leading to the same inverse $\mathbf{G}$). Illustrative examples of solutions that have been considered in the (NIP) and can be cast in this framework are as follows.

1) MN [3], [21], [22]: $\mathbf{W}_e = \mathbf{W}_m = \mathbf{I}$, $\mathbf{I}$ stands for the identity matrix ($\mathbf{I}$).
2) Weighted MN's [4]: $\mathbf{W}_e = \mathbf{I}$ and a diagonal matrix $\mathbf{W}_m$ is introduced to lessen the tendency to superficial reconstructions characteristic of the MN. One example corresponds to choose the ith diagonal element of $\mathbf{W}_m$ as the norm of the ith column of the lead field matrix $\mathbf{L}$ [23].
3) Probabilistic reconstruction of multiple sources (PROM) solution [24]: A method based on the multiple signal classification (MUSIC) algorithm [25] is used to reconstruct the metric matrix $\mathbf{W}_m$.
4) Bayesian approach [26]: $\mathbf{W}_m$ and $\mathbf{W}_e$ are the covariance matrices for the sources and the noise, respectively.
5) Laplacian minimization with column scaling [5]: $\mathbf{W}_e = \mathbf{I}$ and $\mathbf{W}_m = \mathbf{D}^t\mathbf{B}^t\mathbf{B}\mathbf{D}$, where $\mathbf{D}$ is a diagonal matrix and $\mathbf{B}$ is a version of the discrete Laplacian operator.

Appendix II
Some Critical Points of Linear Reconstruction Procedures

Lemma: Let the solution of (1) given by a generalized inverse $\mathbf{G}$ such that $\mathbf{LG} = \mathbf{I}$ and $\mathbf{G} \neq \mathbf{L}^+$ [e.g., as in (AI-5)], then the following statements are true.

1) There are sources $\mathbf{j}^*$ that produce a nonnull measurement vector $\mathbf{m}^*$ and cannot be retrieved by algorithm $\mathbf{G}$.
2) There are sources $\mathbf{j}^*$ that produce a nonnull measurement vector $\mathbf{m}^*$ and fulfill a certain C-ness property ($\mathbf{j}^{*t}\mathbf{C}\mathbf{j}^* \leq \varepsilon$) that cannot be retrieved by the algorithm $\mathbf{G}$ intended to cope with the C-ness property.

Proof: Consider $\mathbf{j}^* = (\mathbf{I} - \mathbf{G}\mathbf{G}^+)\mathbf{h}$ with $\mathbf{h}$ being a nonnull arbitrary vector. By construction, $\mathbf{j}^*$ belongs to the space orthogonal to the columns of $\mathbf{G}$. Thus, there exists no measurement vector $\mathbf{m}$ such that $\mathbf{j}^* = \mathbf{G}\mathbf{m}$. On the other hand, $\mathbf{m}^* = \mathbf{L}\mathbf{j}^* = (\mathbf{L} - \mathbf{G}^+)\mathbf{h}$ will be equal to zero (for any vector $\mathbf{h}$) only when $\mathbf{G} = \mathbf{L}^+$(MN), a condition that does not hold by hypothesis. Then, this source $\mathbf{j}^*$produces a data vector $\mathbf{m}^*$ and cannot be retrieved by $\mathbf{G}$, as stated in 1). To proof 2) consider the source $\alpha\mathbf{j}^*$ with α selected from the condition $\alpha^2\mathbf{j}^{*t}\mathbf{C}\mathbf{j}^* \leq \varepsilon$. In general, all the sources that satisfy either 1) or 2) are linear combinations (with properly chosen coefficients) of the columns of matrix $(\mathbf{I} - \mathbf{G}\mathbf{G}^+)$ that do not belong to Ker($\mathbf{L}$). The existence of such columns follows from the condition $\mathbf{G} \neq \mathbf{L}^+$.

Appendix III
Radial Weighting Strategy

The radial weighting strategy mentioned in Section II-E is based on selecting weights which force the primary current distribution to be zero beyond a certain sphere which defines the brain limits, a physical property that has to be fulfilled by any spatially bounded current distribution. This property, fulfilled by the MN in a physically unsatisfactory way, is here guaranteed by using the simple weighting function $W_{ii} = (1)/(|R - r_i|^n)$ where R is the radius of the sphere beyond which the primary currents have to be zero and r_i stand for the ith solution point. The integer n controls the "velocity of decay" of the currents.

Acknowledgment

The authors would like to thank O. Hauk for his assistance with the figures and Prof. Dr. B. Lütkenhöner for fruitful discussions. They would also like to thank Prof. M. Hoke, Dr. E. Menninghaus, and other members of the Institute for Experimental Audiology for their support. Finally, the authors would like to thank the unknown referees for their invaluable comments and suggestions.

References

[1] J. Sarvas, "Basic mathematical and electromagnetic concepts of the biomagnetic inverse problem," *Phys. Med. Biol. 32*, pp. 11–22, 1987.
[2] J. Malmivuo and R. Plonsey, *Bioelectromagnetism: Principles and Applications of Bioelectric and Biomagnetic Fields.* New York: Oxford Univ. Press, 1995.
[3] M. Hämäläinen and R. Ilmoniemi, "Interpreting magnetic fields of the brain: Minimum norm estimates," *Med. Biol. Eng., Comput.*, vol. 32, pp. 35–42, 1994.
[4] B. Jeffs, R. Leahy, and M. Singh, "An evaluation of methods for neuromagnetic image reconstruction," *IEEE Trans. Biomed. Eng.*, vol. BME-34, pp. 713–723, 1987.
[5] R. D. Pascual-Marqui and C. M. Michel, "Low resolution electromagnetic tomography: A new method for localizing electrical activity in the brain," *Int. J. Psychophysiol.*, vol. 18, pp. 49–65, 1994.
[6] R. M. Leahy, J. C. Mosher, and J. W. Phillips, "A comparative study of minimum norm inverse methods for MEG imaging," in *Proc. 10th Int. Conf. Biomagnetism*, BIOMAG'96, to be published.
[7] G. E. Backus and J. F. Gilbert, "The resolving power of gross earth data," *Geophys. J. Roy. Astron. Soc.*, vol. 16, pp. 69–205, 1968.
[8] W. Menke, *Geophysical Data Analysis: Discrete Inverse Theory.* New York: Academic, 1984.
[9] M. Hämäläinen, R. Hari, R. J. Ilmoniemi, J. Knuutila, and O. V. Lounasmaa, "Magnetoencephalography—Theory, instrumentation and applications to noninvasive studies of the working human brain," *Rev. Modern Phys.*, vol. 65, no. 2, pp. 413–497, 1993.
[10] R. Grave de Peralta, S. Gonzalez, and B. Lütkenhönner, "Figures of merit to compare linear inverse distributed solutions," *Brain Topogr.*, vol. 9, no. 2, pp. 117–124.

[11] R. Grave de Peralta, O. Hauk, S. Gonzalez, H. Vogt, and C. Michel, "Linear inverse solutions with optimal resolution kernels applied to the electromagnetic tomography," *Human Brain Mapping*, vol. 5, pp. 454–467, 1997.
[12] M. Bertero, C. De Mol, and E. R. Pike, "Linear inverse problems with discrete data. I: General formulation and singular system analysis," *Inverse Problem*, vol. 1, pp. 301–330, 1985.
[13] C. de Mol, "A critical survey of regularized inversion methods," in *Inverse Problems in Scattering and Imaging*, M. Bertero and E. R. Pike Eds. Bristol, U.K.: Adam Hilger, 1992, pp. 345–369.
[14] A. K. Louis, "Approximate inverse for linear and some nonlinear problems," *Inverse Problem*, vol. 12, pp. 175–190, 1996.
[15] C. R. Rao and S. K. Mitra, *Generalized Inverse of Matrices and Its Applications*, New York: Wiley, 1971.
[16] G. Wahba, *Spline Models for Observational Data*. Philadelphia, PA, SIAM, 1990.
[17] J. P. Ary, S. A. Klein, and D. H. Fender, "Location of sources of evoked scalp potentials: Corrections for skull and scalp thickness," *IEEE Trans. Biomed. Eng.*, vol. 28, pp. 447–452, 1989.
[18] S. Rush, "On the independence of magnetic and electric body surface recordings," *IEEE Trans. Biomed. Eng.*, vol. BME-22, pp. 157–167, 1975.
[19] C. L. Lawson and R. J. Hanson, *Solving Least Squares Problems*. Engl.wood Cliffs, NJ: Prentice-Hall, 1993.
[20] S. Gonzalez, R. Grave de Peralta, R. Biscay, J. C. Jimenez, R. D. Pascual, J. Lemagne, and P. Valdes, "Projective methods for the magnetic direct problem," in *Advances in Biomagnetism*, S. J. Williamson, M. Hoke, G. Stroink, and M. Kotani, Eds. New York: Plenum, 1989, pp. 615–618.
[21] C. W. Crowley, R. E. Greenblatt, and I. Khalil, "Minimum norm estimation of current distributions in realistic geometries," in *Advances in Biomagnetism*, S. J. Williamson, M. Hoke, G. Stroink, and M. Kotani, Eds. New York: Plenum, 1989, pp. 603–606.
[22] J. Z. Wang, S. J. Williamson, and L. Kaufman, "Magnetic source images determined by a lead-field analysis: The unique minimum-norm least-squares estimation," *IEEE Trans. Biomed. Eng.*, vol. 39, pp. 665–675, 1992.
[23] I. Gorodnitsky, J. S. George, and H. A. Schlitt, "A weighted iterative algorithm for neuromagnetic imaging," in *Proc. IEEE Satellite Symp. Neuroscience and Technology*, Lyon, France, 1992, pp. 60–64.
[24] R. E. Greenblatt, "Probabilistic reconstruction of multiple sources in the neuroelectromagnetic inverse problem," *Inverse Problems*, vol. 9, pp. 271–284, 1993.
[25] J. C. Mosher, P. S. Lewis, and R. M. Leahy, "Multiple dipole modeling and localization from spatio-temporal MEG data," *IEEE Trans. Biomed. Eng.*, vol. 39, pp. 541–557, 1992.
[26] A. M. Dale and M. I. Sereno, "Improved localization of cortical activity by combining EEG and MEG with MRI cortical surface reconstruction: A linear approach," *J. Cogn. Neurosci.*, vol. 5, pp. 162–176, 1993.

Rolando Grave de Peralta-Menendez was born in Santiago de Cuba, Cuba, on November 30, 1962. He received the M.Sc. degree in mechanical engineering (with honors) from the Technical University of Havana (ISPJAE), Havana, Cuba, in 1987 and the M.Sc. degree in mathematics from the University of Havana, Havana, in 1992.

He was Associated Researcher and Assistant Professor at the Cuban National Center for Scientific Research, Havana, Cuba, from 1987 to 1995, when moved to the Institute of Experimental Audiology, University of Muenster, Muenster, Germany. Since 1996 he has been a Specialist on Inverse Problem, at the Functional Brain Mapping Lab, University Hospital of Geneva, Geneva, Switzerland. His research interest centers on applied mathematics, namely, numerical analysis, global optimization techniques, and inverse problems with discrete data and its applications in biomedicine.

Sara L. Gonzalez-Andino was born in Havana, Cuba, on November 8, 1963. She received the M.Sc. degree in physics (with honors) from the University of Havana, Havana, Cuba, in 1985.

She was Associated Researcher and Assistant Professor at the Cuban National Center for Scientific Research, Havana, Cuba, from 1985 to 1995. From 1989 to 1990 she was a Visitor Researcher at the Institute of Experimental Audiology, University of Muenster, Muenster, Germany. Since 1996 has been with the Functional Brain Mapping Lab, University Hospital of Geneva, Geneva, Switzerland. Her research interest include biophysical modeling, inverse and direct problem solution in biomedicine, and studies about coherence and synchrony in the human brain.